Solution of the Riemann problem for water with phase transition: influence of the equation of state

Bertrand Mercier

Solution of the Riemann problem for water with phase transition: influence of the equation of state

Bertrand Mercier CEA/INSTN 91191 Gif sur Yvette cedex
https://orcid.org/0000-0002-3332-9158
Jan 25, 2023 mail to bertrand.mercier@cea.fr

Highlights :

- We solve the Riemann problem for depressurization of water
- For such a problem, the IAPWS equation of state (EOS) can be approximated by a stiffened gas EOS in the pure liquid and/or pure steam phase
- A tabulated EOS can be efficiently used for the diphasic domain

Abstract: We address the solution of the Riemann problem for water in the diphasic domain.
We compare the solution obtained with the IAPWS equation of state (EOS) with the solution obtained with a modified stiffened gas EOS for pure liquid water, a tabulated EOS for the diphasic domain and a modified perfect gas EOS for pure steam. Since our interest is phase transition, we limit ourselves to temperatures below 623 K. We obtain convex isentropes which do not cross each other, so that the Riemann problem can be solved easily and its solution is unique. We analyze the effect of the EOS which has been selected.
We give examples which are useful to understand the depressurization process in a tube.

Keywords: depressurization, diphasic flows, shocks, rarefaction waves, real EOS

1. Introduction

For real materials, the Riemann Problem has been considered in the pioneering work by R. Menikoff & B. Plohr[8]. In particular, they show that when the isentropes in the (τ, p) plane are convex, then the Riemann problem has a unique solution.
As we shall see, for water in the temperature domain we consider, we get convex isentropes.
Indeed, the entropy diagram for water (see e.g.
https://demonstrations.wolfram.com/TemperatureEntropyDiagramForWater/)
shows that, for water, when one follows a given isentrope, the saturation line can be crossed only once: from the liquid to the diphasic domain or from the steam to the diphasic domain.
Since the sound speed is higher in the liquid domain than in the diphasic domain and also higher in the steam domain than in the diphasic domain, we shall deduce that for water, isentropes are convex in the (τ, p) plane.

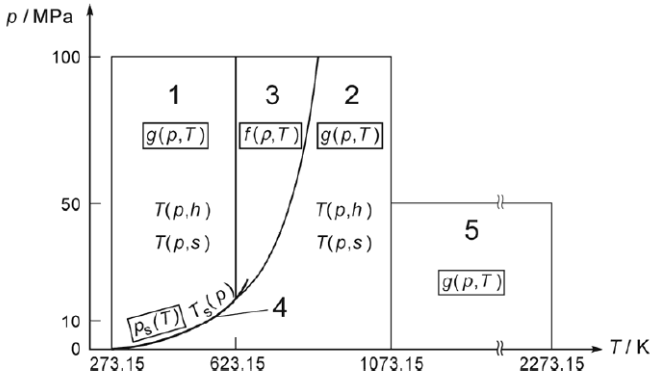

Fig. 1. Regions and equations of IAPWS-IF97.

In [11] Müller & Voss consider so called "retrograde fluids" like dodecane for which this is not the case. In the present paper, we restrict ourselves to water, for which very accurate EOS have been established like IAPWS97 [14]. We shall consider temperatures below 623K, which is a bit smaller than the critical one (647K). As indicated in Fig 1, extracted from [14], we shall need the EOS given by IAPWS for regions 1 (liquid domain), 2 (steam domain) & 4 (diphasic domain).
The IAPWS97 EOS is very accurate, but somewhat costly as regards computing time. See more details in [12]. People frequently use stiffened gas EOS for pure liquid water and another one for pure steam water. Then they apply thermodynamic laws to obtain an EOS in the diphasic domain, as explained in [5, 7]. This induces a computational cost, and this is the reason why people also build look-up tables as in [12] or [13].
In the present paper, we use look-up tables for the diphasic domain only. We complement them by a modified stiffened gas EOS for the pure liquid domain (IAPWS region 1) and a modified perfect gas EOS for pure steam domain (IAPWS region 2).
In §2 we show how to use our table to derive an EOS in the diphasic domain (IAPWS region 4).
In §3, we show how to combine our diphasic EOS with a modified stiffened gas EOS (SG) in the pure liquid domain (IAPWS region 1).
In §4, we show how to combine our diphasic EOS with a modified perfect gas EOS (PG) in the steam domain (IAPWS region 2).
In §5 we address the solution of the Riemann problem with our combined EOS.
We show that the isentropes we obtain in the (τ, p) plane are convex, which, according to [9], proves that the Riemann problem has a unique solution.
Like in [8] we use a graphical method for solving the Riemann problem.
Finally, we give some specific examples in connection with depressurization.

2 Equation of state for diphasic water.

Formalism

In what follows, the subscript f (resp. v) stands for liquid (resp. steam)
For equilibrium diphasic mixtures (steam + liquid) we have extracted from IAPWS a table of 300 lines.
For $1 \leq i \leq 300$, our table gives a value T_i for the saturation temperature and the 7 values $p(T_i)$, $\tau_f(T_i)$, $\tau_v(T_i)$, $\varepsilon_f(T_i)$, $\varepsilon_v(T_i)$, $s_f(T_i)$, $s_v(T_i)$.
We have $T_1 = 335\ K$ and $T_{300} = 634\ K$ which gives limits to our domain of validity.
From our table, following Müller & Voss [11], we proceed in the following way:

Method A: to compute p, T and s, when τ and ε are given: Let

$$y_\tau(T) = \big(\tau - \tau_v(T)\big)/\Big(\tau_f(T) - \tau_v(T)\Big)$$
$$y_\varepsilon(T) = \big(\varepsilon - \varepsilon_v(T)\big)/\Big(\varepsilon_f(T) - \varepsilon_v(T)\Big)$$

To compute T we just have to solve the equation $y_\tau(T) = y_\varepsilon(T)$.
This is a nonlinear equation with one unknown T which can be easily solved by

- finding i such that $y_\tau(T_i) > y_\varepsilon(T_i)$ and $y_\tau(T_{i+1}) < y_\varepsilon(T_{i+1})$
- solving a second-degree equation to find θ such that $T = (1-\theta)T_{i+1} + \theta T_i$ and $\big(\tau - \tau_v(T)\big)\Big(\varepsilon_f(T) - \varepsilon_v(T)\Big) = \big(\varepsilon - \varepsilon_v(T)\big)\Big(\tau_f(T) - \tau_v(T)\Big)$
- From the value of θ, compute $T = (1-\theta)T_{i+1} + \theta T_i$ and then p (which depends on T).
- Let y^* denote the common value of $y_\tau(T)$ and $y_\varepsilon(T)$ we let $s = y^*\ s_f(T) + (1-y^*)\ s_v(T)$ ■

Method B: to compute p, T and ε, when τ and s are given:

In the same way, we solve $y_\tau(T) = y_s(T) = y^*$ where

$$y_\tau(T) = \big(\tau - \tau_v(T)\big)/\Big(\tau_f(T) - \tau_v(T)\Big)$$

$$y_s(T) = \big(s - s_v(T)\big)/\Big(s_f(T) - s_v(T)\Big)$$

The details are left to the reader. ■

Evaluation of isentropes.

With method B it is very easy to plot an isentrope.

With method A, we proceed by increment. If we start from $\big(\tau, \varepsilon, p(\tau, \varepsilon)\big)$ we move to $\big(\tau + d\tau, \varepsilon + d\varepsilon, p(\tau + d\tau, \varepsilon + d\varepsilon)\big)$ by choosing $d\varepsilon = -pd\tau$

On Fig 2 we start from $\tau = 363.21$ L/kg, with $s = 2.661$ kJ/kg/K ; for method A we take $d\tau = -3$ L/kg and we check that at the end of the curve ($\tau = 3.21$ L/kg), we obtain $s = 2.653$ kJ/kg/K that is a relative error of 0.3%. Of course, such an error decreases if we decrease $d\tau$.

We give both results on Fig 2.

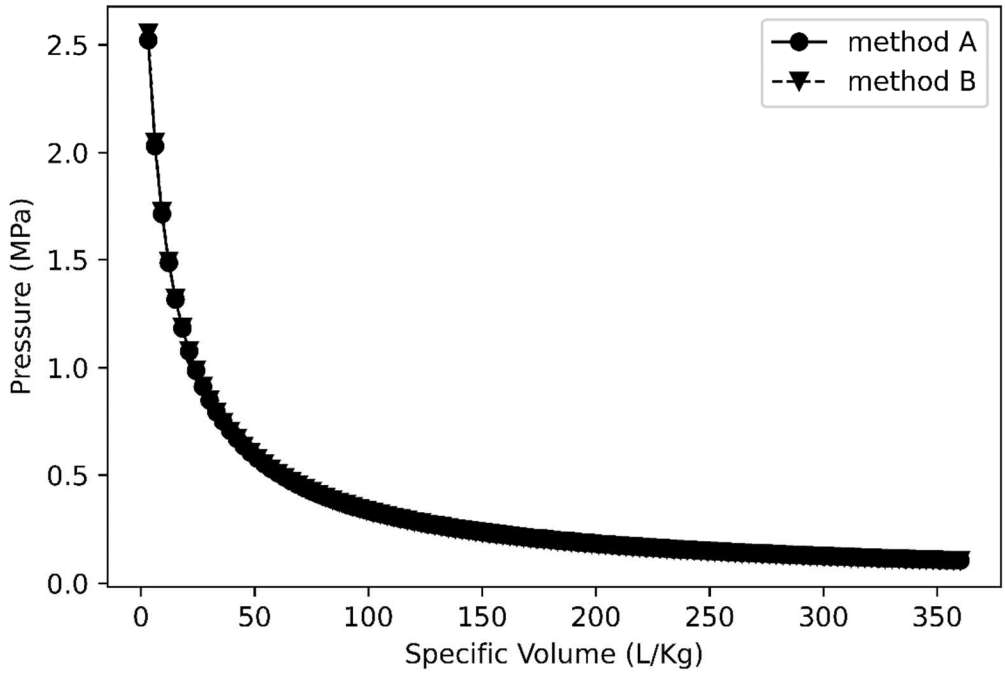

Fig 2. Isentropic curve starting from $\tau = 363.21$ L/kg, with $s = 2.661$ kJ/kg/K computed with methods A vs B

Sound speed

If we use τ, s as the primitive variables, so that we can use Method B, we have

$$c = \tau\sqrt{-\partial p/\partial \tau} \qquad (1)$$

With τ, ε as the primitive thermodynamic variables, we can use Method A and

$$c = \tau\sqrt{p.\partial p/\partial \varepsilon - \partial p/\partial \tau} \qquad (2)$$

In the following test we replace partial derivatives by finite differences, and we get the results given in Fig 3 for $p = 12.9$ MPa. Note that we obtain 2 superposed curves.

This proves that both methods are valid. As we shall see, Method A (and then (1)) is useful for solving the Riemann problem. Method B (and then (2)) is useful for Finite Volume codes.

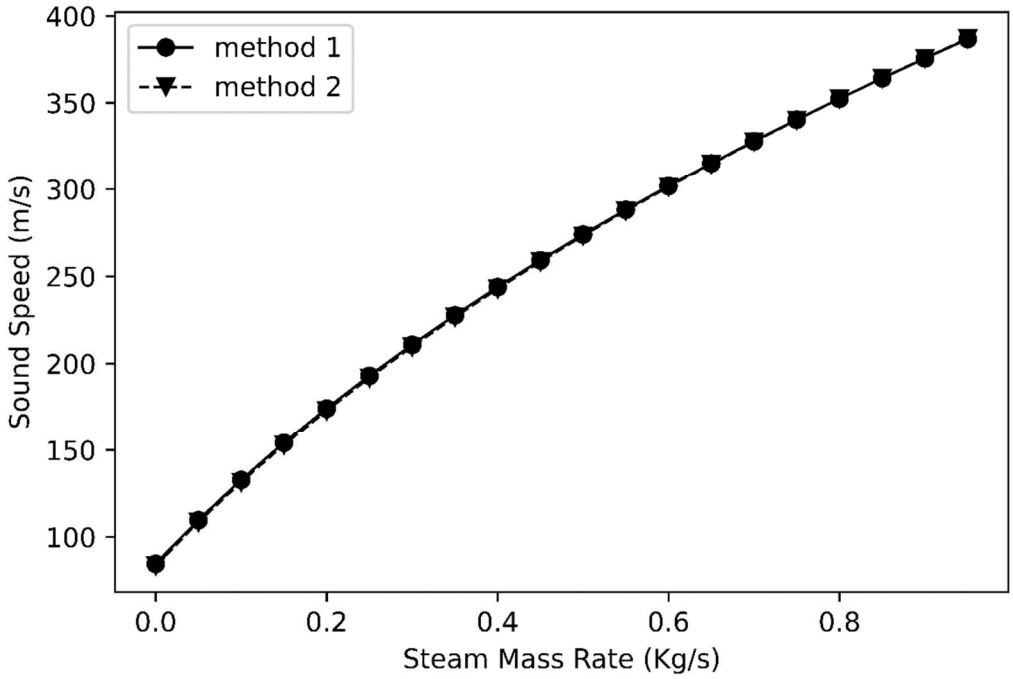

Fig 3 Sound speed evaluated either with (1) or (2) as a function of the steam mass rate x

We notice that the sound speed in a diphasic mixture is much lower than in the liquid phase, where it is of the order of 800 to 1500 m/s. This result is well known.

3 Equation of state for the liquid phase

For the pure liquid phase, we shall use a stiffened gas (SG) EOS.[5]

$$p = -\gamma p_\infty + (\gamma - 1)(\varepsilon - q)/\tau \qquad (3)$$

However, in the standard stiffened gas model, q is a constant, whereas here we shall require that

$$p = -\gamma p_\infty + (\gamma - 1)(\varepsilon - q)/\tau_f(p)$$

on the saturation line $p, \tau_f(p), \varepsilon_f(p)$, which means that we shall select

$$q = q(p) = \varepsilon_f(p) - (p + \gamma p_\infty)\tau_f(p)/(\gamma - 1))$$

This is necessary to define a continuous (but not differentiable) value of ε across the saturation line. More precisely, for a given point in the pure liquid domain (τ, p), we first determine a point (τ_0, p_0) on the saturation line such that,

$$p + p_\infty = (p_0 + p_\infty)\,(\tau_0/\tau)^\gamma \qquad (4)$$

$$\tau_0 = \tau_f(p_0)$$

Then we compute

$$q = \varepsilon_f(p_0) - (p_0 + \gamma p_\infty)\tau_0/(\gamma - 1)$$

And finally, we compute $\varepsilon = f(\tau, p)$ by using (4).

In table 1 we compare the specific internal energy obtained with our method, with $\gamma = 2.79$ and $p_\infty = 186$, and the one given by IAPWS97.

The results are given along an isochore line τ =1.4877 L/kg

We note that the results are very close to each other.

We also note that the parameter q is almost constant

P	ε_{IAPWS}	ε_{SG}	q
10.979	1.433	1.433	0.993
11.382	1.434	1.434	0.993
11.784	1.436	1.435	0.994
12.186	1.437	1.436	0.995
12.588	1.439	1.438	0.996
12.990	1.440	1.439	0.997
13.392	1.441	1.440	0.997
13.794	1.443	1.441	0.998
14.196	1.444	1.442	0.999
14.598	1.445	1.443	1.000
15.000	1.447	1.444	1.000

Table 1 IAPWS Specific energy vs SG specific energy for τ =1.4877 L/kg

Note that there are some points (τ, p) in the liquid domain for which we shall not be able to find (τ_0, p_0)**.** Let (τ_{min}, p_{min}) denote the smallest point on the saturation line in our table this will be the case for the points on the left of the isentropic curve $p + p_\infty = (p_{min} + p_\infty)\ (\tau_{min}/\tau)^\gamma$. For these points we select $q = q_{min} = \varepsilon_f(p_{min}) - (p_{min} + \gamma p_\infty)\tau_{min}/(\gamma - 1)$
This gives an EOS which is incomplete in the sense of Menikoff-Plohr, but can be completed as indicated in [8].

To evaluate an isentrope with such an EOS, we can proceed in the following way:

- We start from (τ, ε, p) satisfying $\varepsilon = f(\tau, p)$
- We introduce increments $(d\tau, d\varepsilon, dp)$ satisfying both
- $d\varepsilon = f_\tau d\tau + f_p dp$ and
- $d\varepsilon = -pd\tau$

We easily find a relation between dp and $d\tau$, which allows to evaluate the isentropic curve by increment.
More explicitly, we have

$$(p + p_\infty)\ \tau^\gamma = (p_0 + p_\infty)\ (\tau_0)^\gamma$$

$$\varepsilon = q + \big((p+\gamma p_\infty)\tau\big)/(\gamma - 1)$$

$$\gamma(p + p_\infty)\ \tau^{\gamma-1}d\tau + \tau^\gamma dp = \gamma(p_0 + p_\infty)\ (\tau_0)^{\gamma-1}d\tau_0 + (\tau_0)^\gamma dp_0 \quad \text{(a)}$$

$$d\tau_0 = \frac{d\tau_f}{dp_0}dp_0 \quad \text{(b)}$$

$$d\varepsilon = dq + \big((p+\gamma p_\infty)\ d\tau + \tau\ dp\big)/(\gamma - 1) \quad \text{(c)}$$

$$dq = \frac{d\varepsilon_f}{dp_0}dp_0 - \big((p_0 + \gamma p_\infty)d\tau_0 + \tau_0 dp_0\big)/(\gamma - 1) \quad \text{(d)}$$

$$d\varepsilon = -pd\tau \quad \text{(e)}$$

The unknowns are $d\tau, dp, d\tau_0, dp_0, d\varepsilon, dq$ and we have 5 equations. If we prescribe $d\tau$ we can evaluate dp like the 4 other unknowns.
Proof: Let $= \frac{d\tau_f}{dp_0}$, $b = \frac{d\varepsilon_f}{dp_0}$ $A = b\ - \big((p_0 + \gamma p_\infty)a + \tau_0\big)/(\gamma - 1)$ and $B = \tau\ /(\gamma - 1)$.
Using (c) +(d) +(e), we find that $A\ dp_0 + \ B\ dp = -\frac{\gamma}{\gamma-1}(\ p + p_\infty)\ d\tau$
On the other hand, let $C = \gamma(p_0 + p_\infty)(\tau_0)^{\gamma-1}a\ + (\tau_0)^\gamma$ and $D = -\tau^\gamma$ using (a)+(b) we find that $C\ dp_0 + D\ dp = \gamma(p + p_\infty)\ \tau^{\gamma-1}d\tau$. When $d\tau$ is prescribed
$\begin{pmatrix} dp_0 \\ dp \end{pmatrix}$ is solution of a linear system whose matrix is $\begin{pmatrix} A & B \\ C & D \end{pmatrix}$.

We find numerically that $A.D - B.C \neq 0$. ■

Proposition 1: *Along an isentrope, we have* $dp_0 = d\tau_0 = dq = 0$

Proof: (a) gives

$$\gamma(p + p_\infty)\,\tau^{\gamma-1}d\tau + \tau^\gamma dp = 0 \text{ i-e}$$

$$\gamma(p + p_\infty)\,d\tau + \tau dp = 0$$

(c) + (e) give

$$-pd\tau = \big((p+\gamma p_\infty)\,d\tau + \tau\,dp\big)/(\gamma - 1)$$

i-e

$$(\gamma - 1)pd\tau + (p+\gamma p_\infty)\,d\tau + \tau\,dp = 0$$

which is equivalent. ■

It follows that in the (τ, p) plane, the isentropes for our EOS satisfy (4)

It also follows that the sound speed can be computed by the well-known formula

$$c = \sqrt{\gamma(p+p_\infty)\tau}$$

To adjust the parameters γ and p_∞ of our SG EOS it is desirable to have a look at the sound speed as illustrated in Table 2

We also check that the isentropes do not cross each other in IAPWS region 1.

Tsat (K)	Psat (Mpa)	c IAPWS (m/s)	γ	p_∞ (Mpa)	c SG (m/s)
422	0.46	1468	3	650	1458
491	2.23	1271	3	453	1273
545	5.66	1052	3	277	1053
591.1	10.98	807	2.79	186	904
591.1	10.98	807	2.75	150	812

Table 2 liquid domain sound speed IAPWS vs SG for different SG parameters

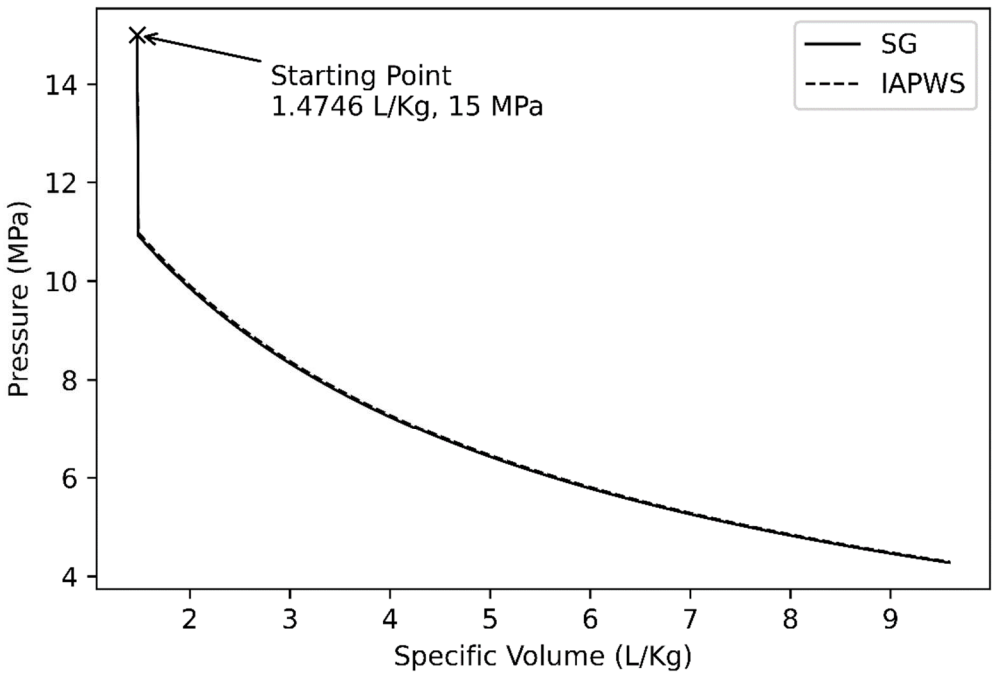

Fig 4. IAPWS vs SG isentrope with $\gamma = 2.79$ and $p_\infty = 186$

On Fig 4, we draw the isentrope starting from $p_0 = 15$ MPa and $\tau_0 = 1.4746$ L/kg in the liquid domain. We complement our isentrope in the two-phase mixture domain by using method B previously described in §2.
We compare the IAPWS isentrope with the SG isentrope with $\gamma = 2.79$ and $p_\infty = 186$.
Even though this is not supposed to be the optimal choice, according to Table 1, we see on Fig 4 that both isentropes are close to each other.
Note that the IAPWS isentrope crosses the saturation line at P=10.97 MPa, $\tau = 1.4877$ L/kg while the SG isentrope crosses it at P=10.92 MPa, $\tau = 1.4855$ L/kg so that the accuracy is acceptable.
Obviously, in both cases, our isentrope is continuous but there is a strong slope discontinuity between both domains.
This corresponds to a strong discontinuity of the sound speed c. Note that such an isentrope is convex. It has a slope discontinuity on the saturation line. But since the slope depends on c^2 and since c decreases, the isentrope is globally convex.

4 Equation of state for the steam phase

First, we recall that, for water, on both sides of the steam saturation line, the sound speed is always higher on the pure steam side. Here is what we get with IAPWS on Fig 5.

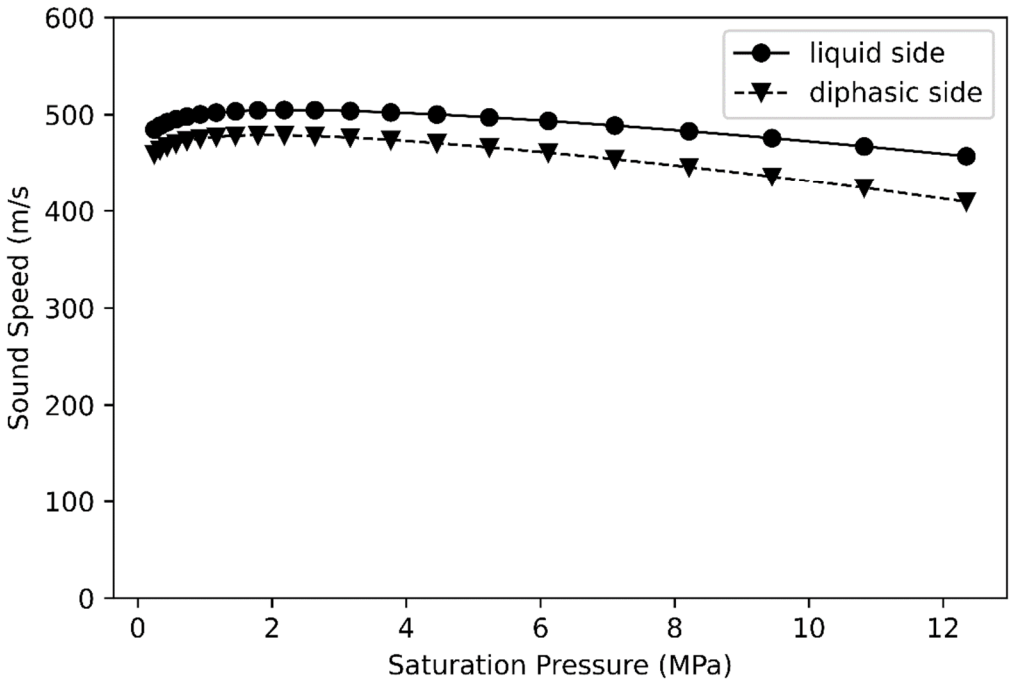

Fig. 5 sound speed c on both sides of saturation line

Since c^2 gives the slope of the isentrope in the (τ, p) plane, this proves that the isentropes are convex. For the pure steam phase, we shall approximate the IAPWS EOS for region 2 by a perfect gas EOS. More precisely we still use (3), but with $p_\infty = 0$.

On Fig 6, we compare the sound speed along the saturation line but on the steam side with IAPWS. The results show that $\gamma = 1.26$ is better at low pressure, and $\gamma = 1.28$ at higher pressures.

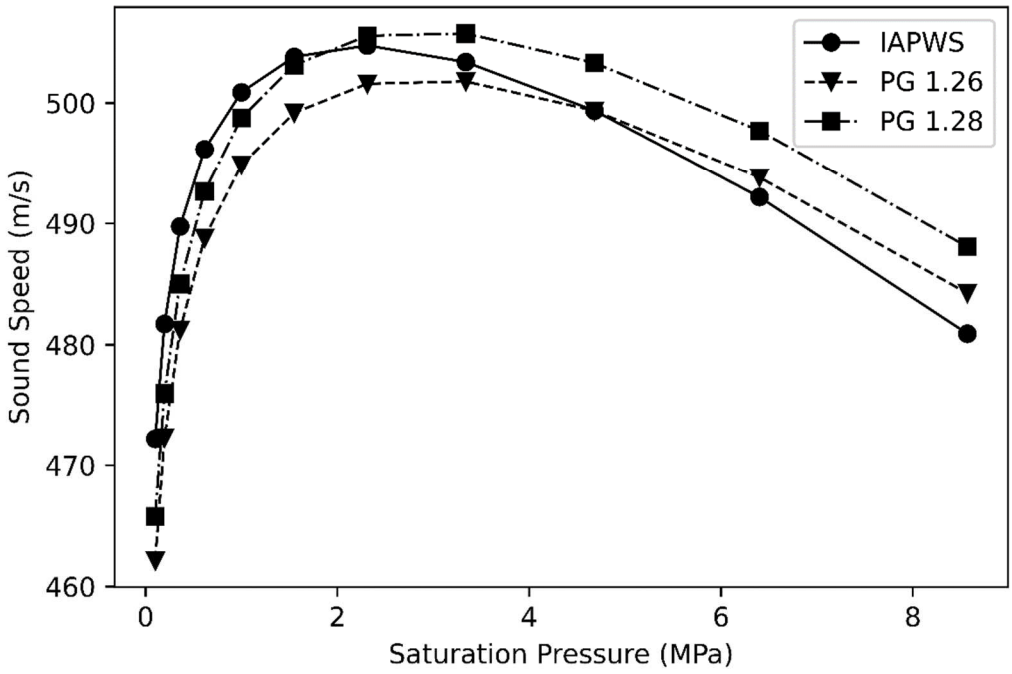

Fig 6 IAPWS vs PG sound speed along the saturation line (steam side)

On Fig 7, we can check that, with the perfect gas (PG) EOS and $\gamma = 1.26$, we get a pretty good approximation to the IAPWS isentrope.

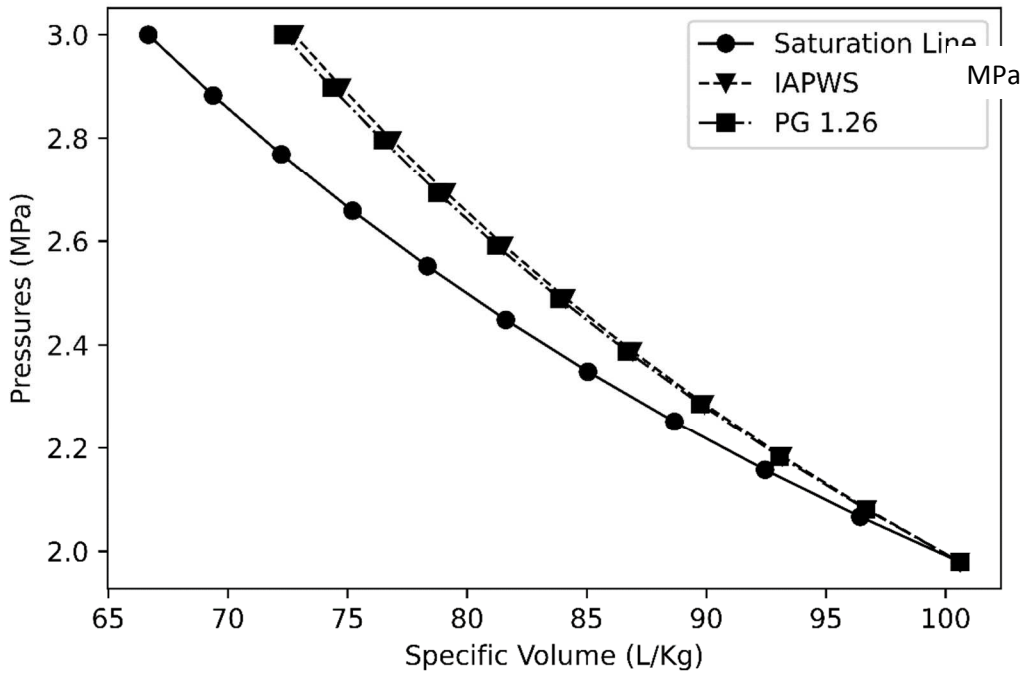

Fig 7 Isentropes on the steam side and saturation line

At $\tau = 34.535\text{L/kg}$, $p = 5.664$ MPa the isentrope is shown on Fig.8.

Note that for $p > 5.664\ MPa$ we are in the pure steam domain and for $p < 5.664\ MPa$ in the diphasic domain.

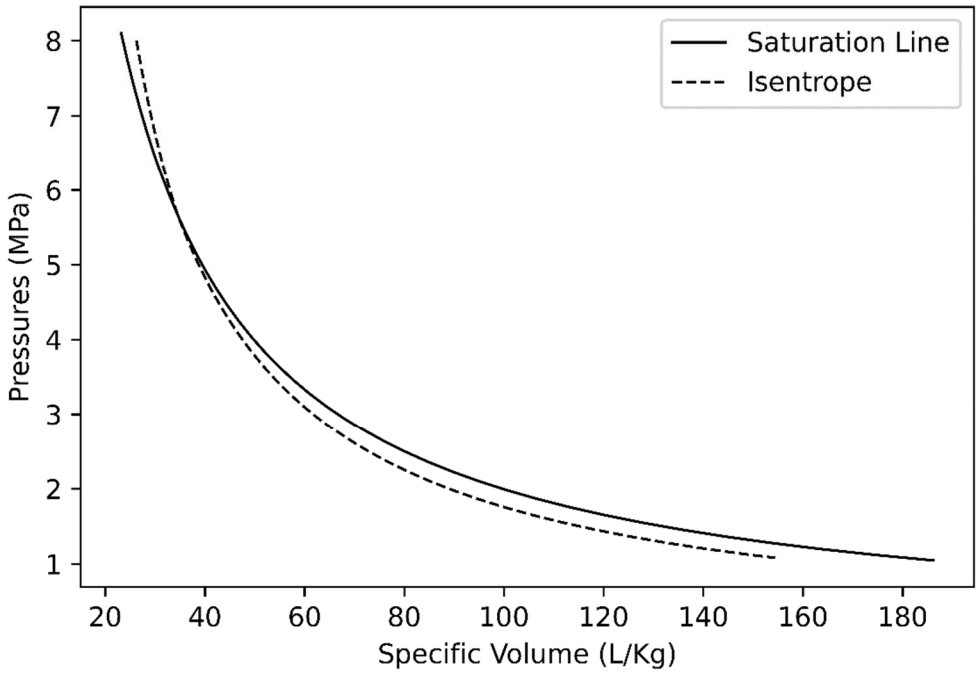

Fig 8 Isentropic curve crossing the steam saturation line at $\tau = 34.535\text{L/kg}$, $p = 5.664\ \text{MPa}$

5: Solution of the Riemann problem

We shall consider the case where we have the same fluid with two different states separated by a diaphragm which is to be removed at time $t = 0$.

u_L, p_L, τ_L	u_R, p_R, τ_R

We then have $u_R = u_L = 0$ and we shall assume that $p_R > p_L$.

We anticipate that we shall have a 1-shock (propagating to the left) and a 3-rarefaction wave propagating to the right.

For $t > 0$ we shall have an intermediate constant state u_* , p_*, itself subdivided in 2 parts separated by a contact discontinuity. On the left (resp. on the right) of the contact discontinuity, we shall have $\tau = \tau_1$ (resp. $\tau = \tau_2$).

We have 4 unknowns u_* , p_*, τ_2, τ_1, and we need 4 scalar equations.

First, let $g(\tau) = \int_{\tau_0}^{\tau} c_R(\sigma)/\sigma \, d\sigma$ and $c_R(\tau) = c(\tau, s_R)$, we shall use the fact that not only the entropy s but also the Riemann invariant $R = u - g(\tau)$, is constant along a 3-rarefaction wave.

We refer the reader e.g. to [4].

We now get our first two equations:

$$u_* - g(\tau_2) - \big(u_R - g(\tau_R)\big) = 0 \qquad (5)$$

$$p_* - f(\tau_2, s_R) = 0 \qquad (6)$$

where the latter gives the isentrope associated to the right state.

We have seen on Fig.4 that we can replace the IAPWS isentrope by a SG isentrope with a good approximation. This is also true in the (u, p) plane as described by (5): see Fig. 9.

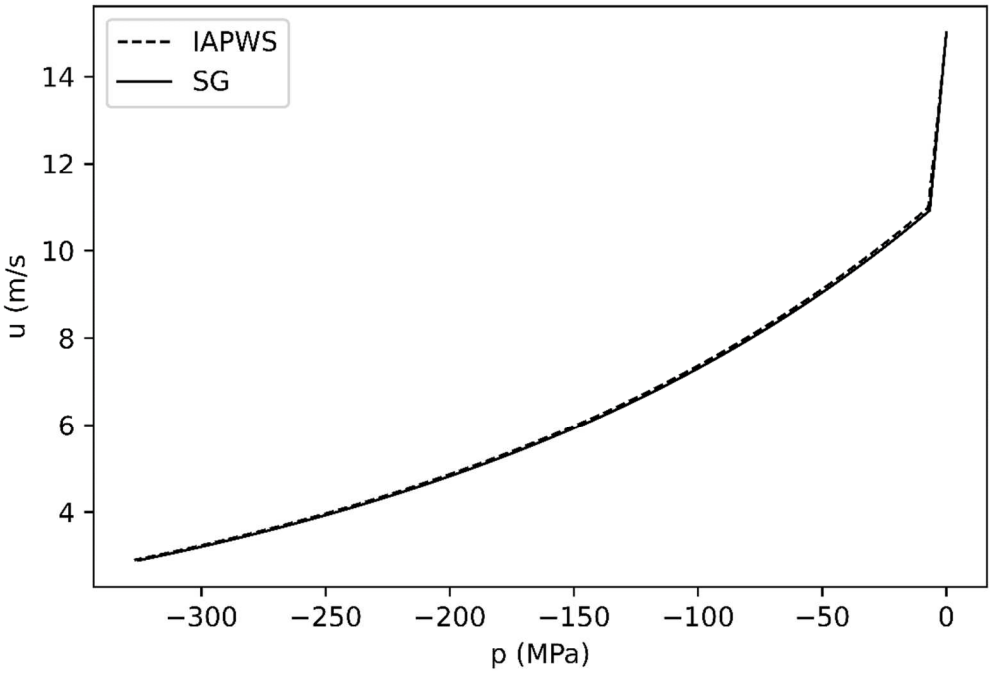

Fig. 9 Rarefaction wave starting from $p_R = 15$ MPa, $\tau_R = 1.4746$ L/kg, $u_R = 0$

Hugoniot curves.

Now what happens along the 1-shock?

Proceeding as DESPRÉS B. [4, p.155], we obtain:

$$(\varepsilon_1 - \varepsilon_L) + \frac{1}{2}(p_1 + p_L)(\tau_1 - \tau_L) = 0 \qquad (7)$$

Since $\varepsilon_1 = f(\tau_1, p_1)$ equation (7) defines a (so called Hugoniot) curve in the plane (τ, p).

This gives our third equation. We denote by

$$p_1 = p_{HO}(\tau_1)$$

the relation we just obtained between p_1 et τ_1.

Remark 1: To obtain the Hugoniot curve in the (u, p) plane we simply use the relation between the jumps across the shock $[p][\tau] + [u]^2 = 0$. It gives our fourth equation.■

Examples of Hugoniot curves

An example is shown in [8] where the Hugoniot curves both in the $\{\tau, p\}$ plane and the $\{u, p\}$ plane are not convex. This is what we find in one case (see Fig.13), in the $\{\tau, p\}$ plane but not in the $\{u, p\}$ plane.

We shall consider 3 cases:

1. Case 1, where the Hugoniot curve starts from $\{\ 315\ \text{L/kg}, 0.6\ \text{MPa}\}$ on the saturation curve and stays in the steam domain
2. Case 2, where the Hugoniot curve is crossing the saturation curve on the steam side, in $\{\ 34.53\ \text{L/kg}, 5.664\ \text{MPa}\}$
3. Case 3, where the Hugoniot curve is crossing the saturation curve on the liquid side in $\{\ 1.3083\ \text{L/kg}, 5.664\ \text{MPa}\}$.

On Fig 10 we compare the Hugoniot curve obtained with IAPWS and the same given by a perfect gas EOS with $\gamma = 1.26$ and $\gamma = 1.28$. The latter gives a slightly better approximation. It seems due to the fact that $\gamma = 1.28$ gives a better approximation to the sound speed for $p < 3$ MPa.

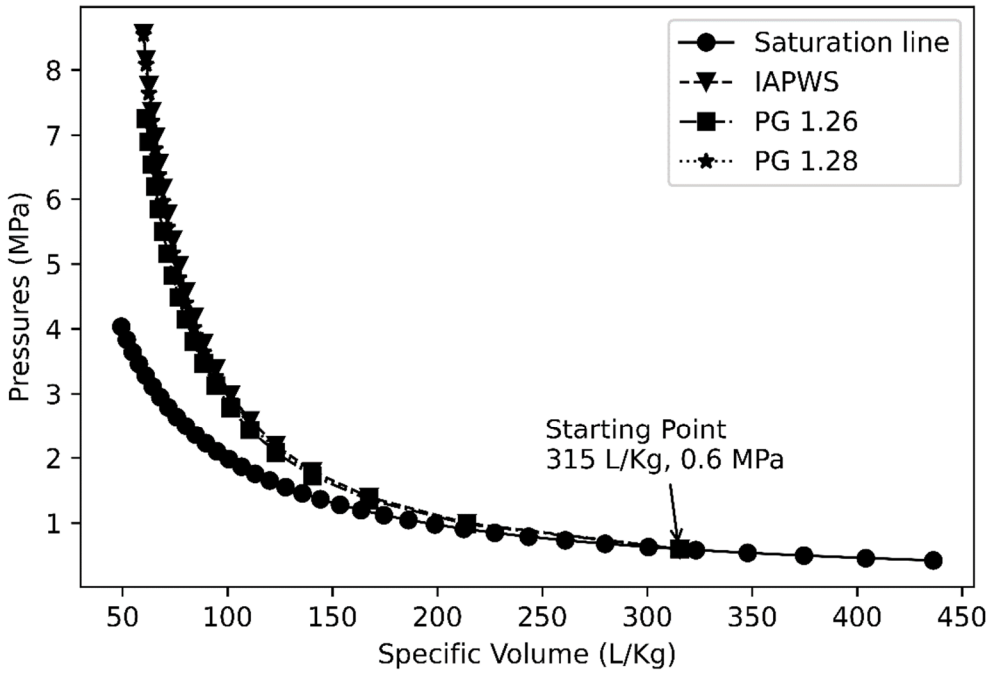

Fig 10 Hugoniot curve starting from the saturation line (case 1)

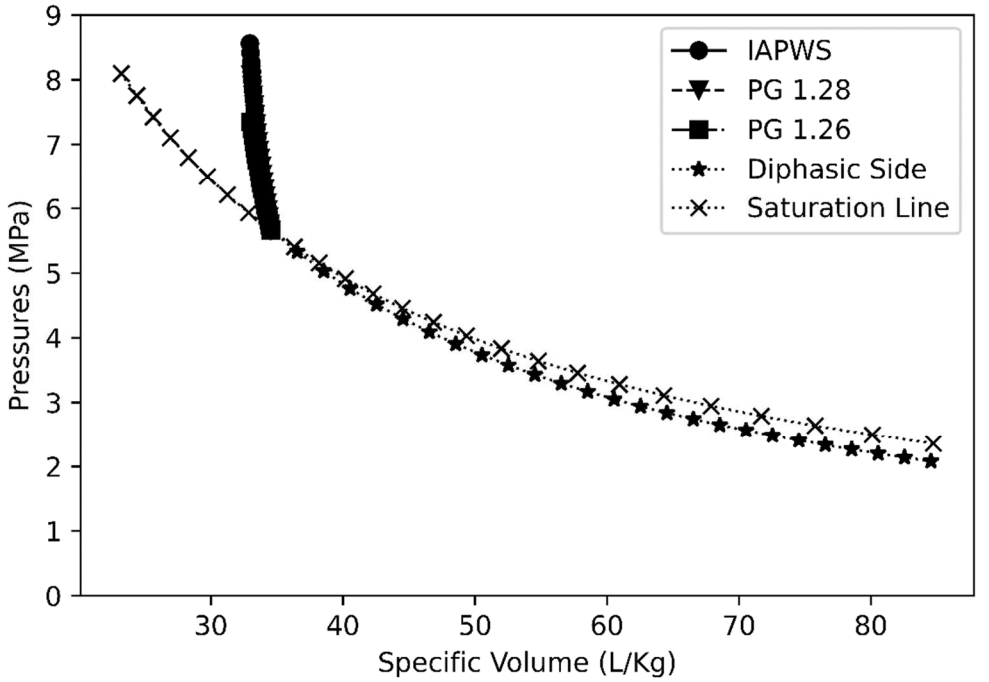

Fig 11 Hugoniot curve crossing the steam saturation line. Case 2.

On Fig 11 we plot (Case 2) the Hugoniot curve starting from $\tau_L = 234\ L/kg$, $p_L = 0.554\ MPa$ inside the diphasic domain. It crosses the saturation line in $\tau = 34.53\ L/kg$, $p = 5.664\ MPa$, and it continues (even though much stiffer) in the pure steam domain.

We make a zoom on the pure steam domain on Fig 12. It shows that the parameter γ is sensitive on this case. The trend is correctly represented with $= 1.28$; not quite so with $\gamma = 1.26$.

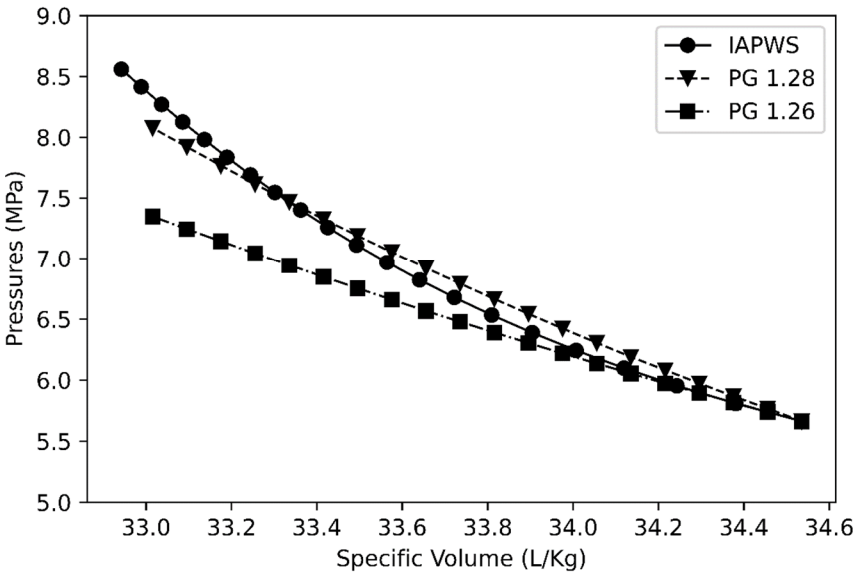

Fig 12 Case 2: Zoom on the Hugoniot curve in the pure steam domain

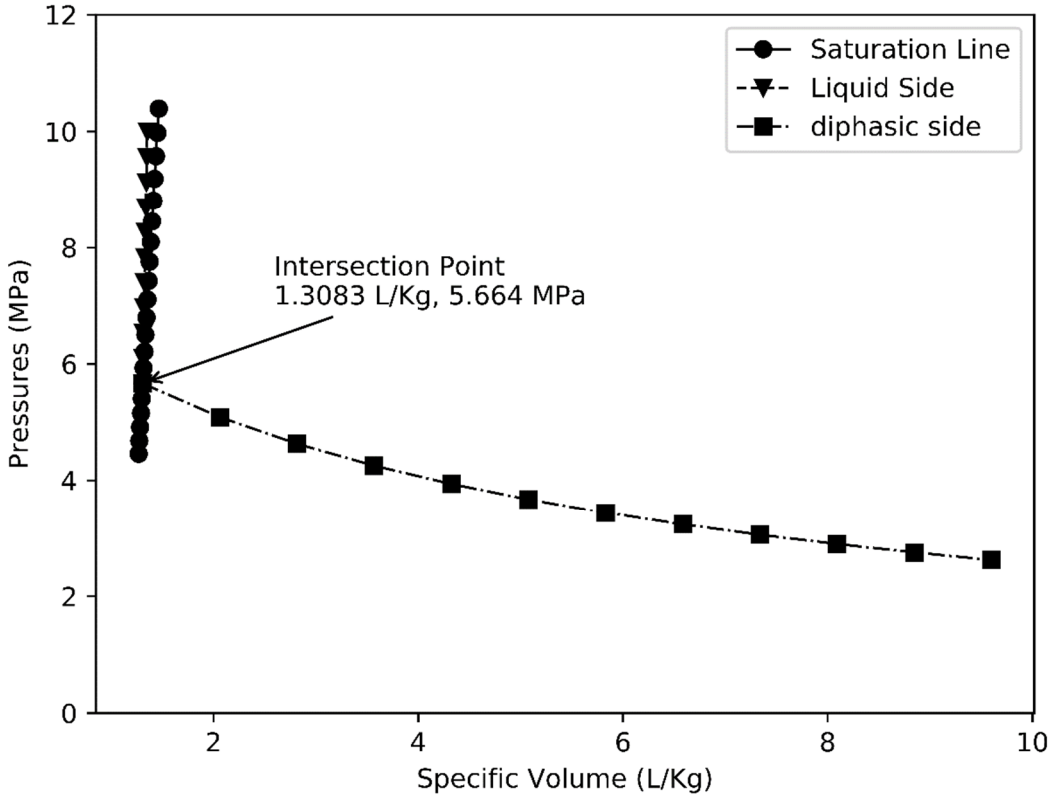

Fig 13 Hugoniot curve crossing the liquid saturation line. Case 3.

We represent the Hugoniot curve starting from $\{\tau_L = 39\ L/kg\ , p_L = 0.894\ MPa\}$ on Fig 13. It crosses the saturation line in $\{\tau_{sat} = 1{,}3083\ \text{L/kg}, p_{sat} = 5.664\ \text{MPa}\}$ (case 3).
Note that for $p < p_{sat}$, τ is decreasing w.r.t p, whereas for $p > p_{sat}$, τ is increasing. In other words two values of the pressure may correspond to the same value of τ.

We found that we get a very good approximation of the Hugoniot curve in the liquid domain, (provided we remain in IAPWS Region 1) if we replace the IAPWS EOS by a SG EOS with $\gamma = 2.79$ and $p_\infty = 186$ MPa or even with $\gamma = 3$ and $p_\infty = 277$ MPa.
Note that the points $\{\tau, p\}$ in the liquid domain should satisfy

$$(\varepsilon - \varepsilon_L) + \frac{1}{2}(p + p_L)(\tau - \tau_L) = 0$$

with the SG approximation, we get
$\varepsilon = q + (p + \gamma p_\infty)\tau/(\gamma - 1))$
That is (after some easy calculations):

$$p = \frac{\varepsilon_L - q - \frac{\gamma p_\infty \tau}{\gamma - 1} - \frac{1}{2}p_L(\tau - \tau_L)}{\frac{\tau}{\gamma - 1} + \frac{1}{2}(\tau - \tau_L)}$$

And we see that the denominator vanishes for $\tau = \tau^*$ with $\tau^* = \frac{\gamma - 1}{\gamma + 1}\tau_L$. In other words we should get that $\tau \to \tau^*$ when $p \to \infty$ (which we can do with the SG EOS). In our case $\tau_L = 39$ L/kg then $\tau^* = 18.4$ L/kg for $\gamma = 2.78$. This explains why τ *increases* from the saturation value 1.3083 L/Kg in the liquid domain.

From the Hugoniot curve $\tau \to p_{HO}(\tau)$ we can deduce another Hugoniot curve in the $\{u, p\}$ plane by
$\tau \to \{u_{HO}(\tau)\ , p_{HO}(\tau)\ \}$ with
$u_{HO}(\tau) = u_L - \sqrt{(\tau_L - \tau)(p_{HO}(\tau) - P_L)}$

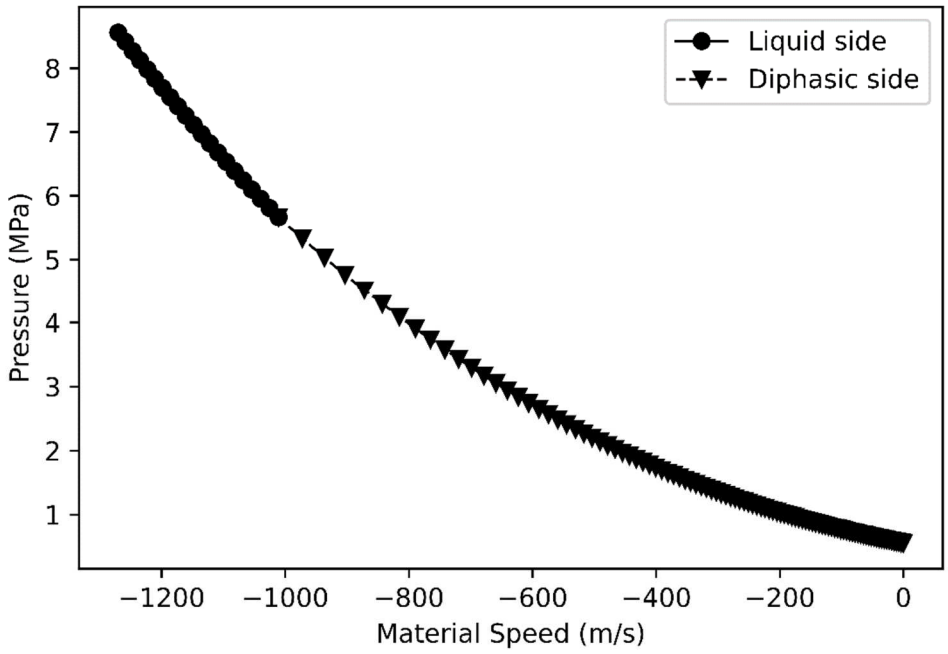

Fig 14 Hugoniot curve in $\{u, p\}$ axes for case 2.

On Fig *14*, we plot the Hugoniot curve in $\{u, p\}$ axes. We represent The IAPWS curve with circles (resp. triangles) in the liquid (resp. diphasic) domain.

Graphical solution to the Riemann problem

To graphically solve the Riemann problem, we just have to find the intersection in the $\{u, p\}$ plane of the isentropic curve starting from the state $\{\tau_R, p_R, u_R\}$ and the Hugoniot curve starting from the state $\{\tau_L, p_L, u_L\}$.

Here is an example: we take $\{39\,\mathrm{L/kg},\ 0.894\ \mathrm{MPa}, 0\ \mathrm{m/s}\}$ on the left and $\{1.4746\,\mathrm{L/kg},\ 15\mathrm{MPa}, 0\ \mathrm{m/s}\}$ on the right. Here is what we get on Fig 15.

The intersection is obtained for $p^* \cong 3.51\ \mathrm{MPa}$ and $u_* \cong -290.9\ \mathrm{m/s}$.

This corresponds to $\tau_2 \cong 13.3\,\mathrm{L/kg}$ on the isentrope and $\tau_1 \cong 5.2\,\mathrm{L/kg}$ on the Hugoniot.

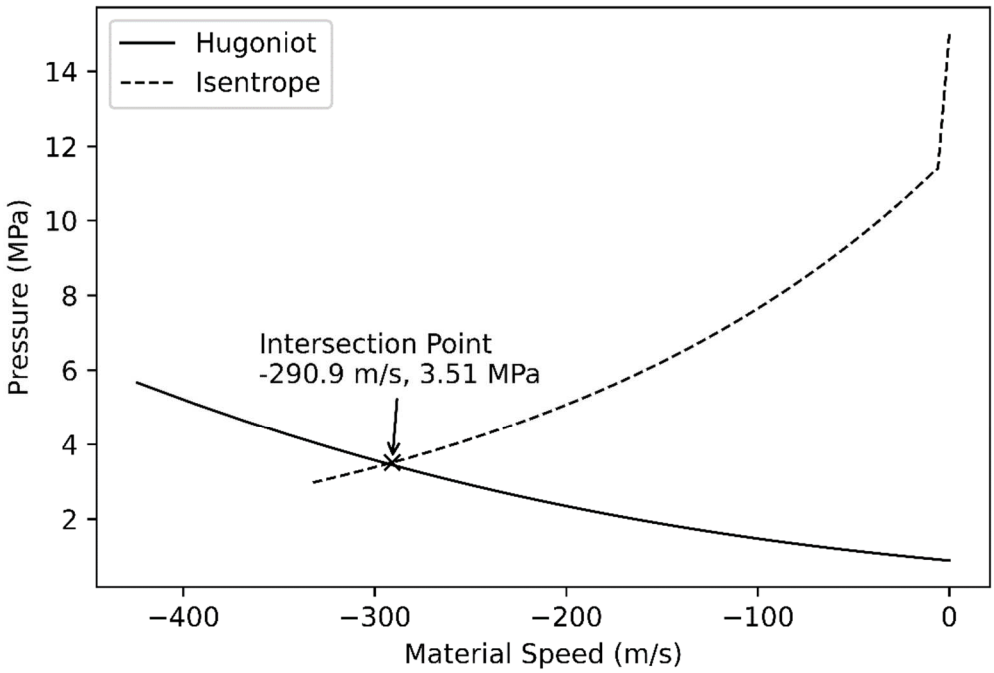

Fig 15: Graphical solution to the Riemann Problem in a $\{u, p\}$ diagram

On Fig 16 to 18, we give a plot of the solution of this Riemann problem at t = 2.5ms.

We compare the IAPWS solution to the SG solution with $\gamma = 2.39, p_\infty = 186\ \mathrm{MPa}$.

We notice a slight discrepancy. It comes when we replace the IAPWS rarefaction curve in dashed line on Fig 15 by the SG rarefaction curve appearing on Fig. 9.

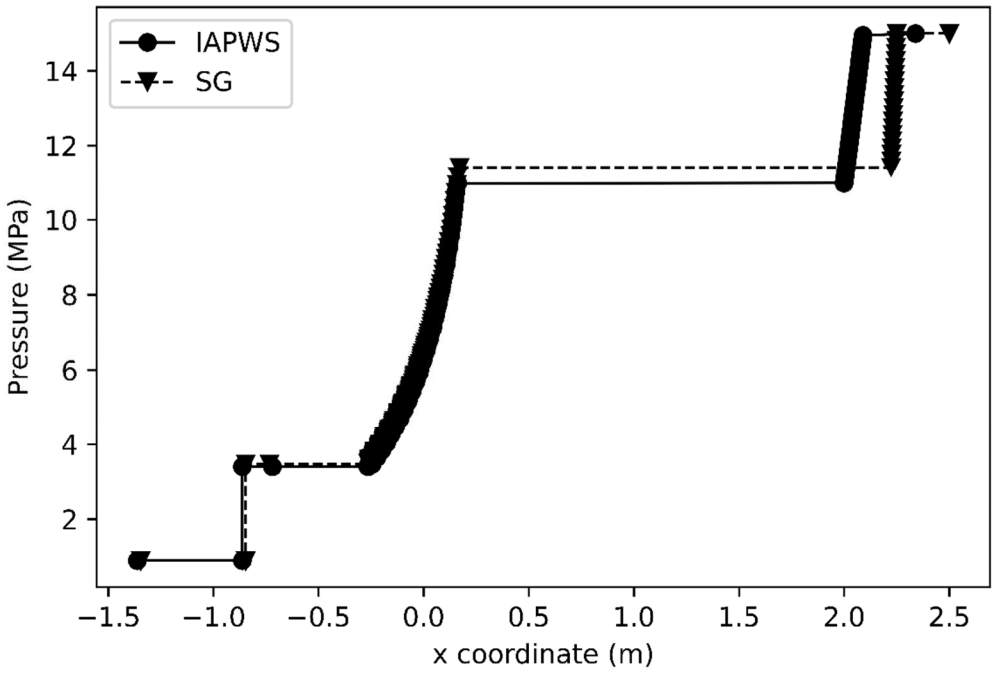

Fig 16 Solution to the Riemann Problem at *t*=2.5 ms. *Pressure in* MPa *wrt x (*m*).*

We notice that the rarefaction wave is made of 2 parts: the first one propagates rapidly (900 m/s) to the right and decreases the pressure from 15 MPa to 10.97 MPa, that is the saturation pressure located on the same isentropic curve as $\{\tau_R, P_R\}$. The second part is relatively slow (~68 m/s) and decreases from 10.97 MPa to 3.48 MPa. We can say that there is a fast depressurization, which hardly decreases the volumic mass, followed by a slow depressurization.

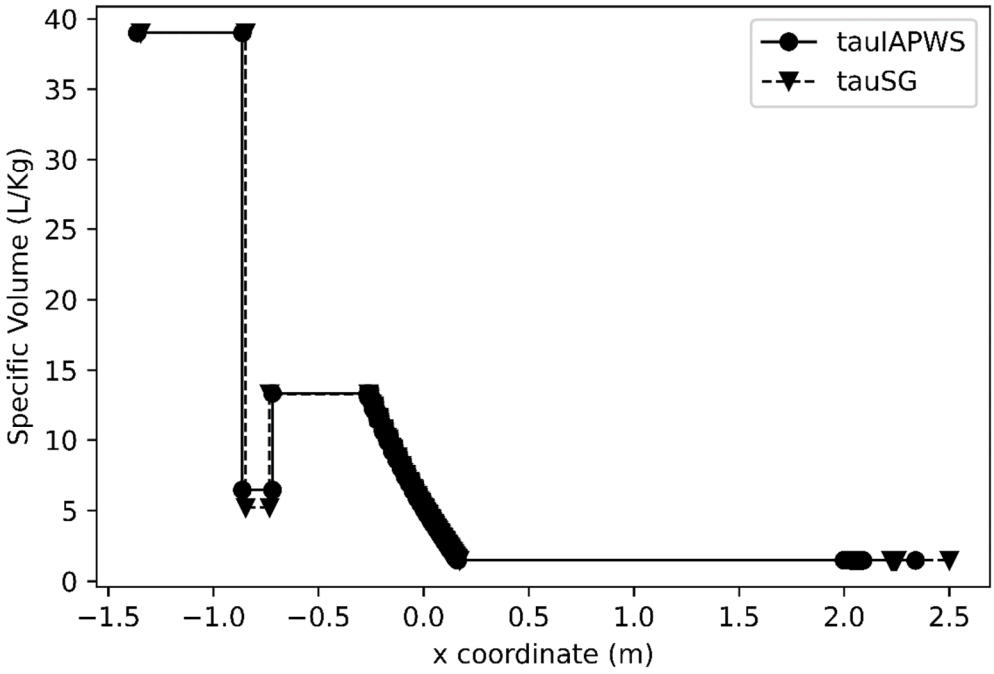

Fig 17 Solution to the Riemann Problem at *t*=2.5 ms. Specific volume (L/kg*)* wrt *x (*m*).*

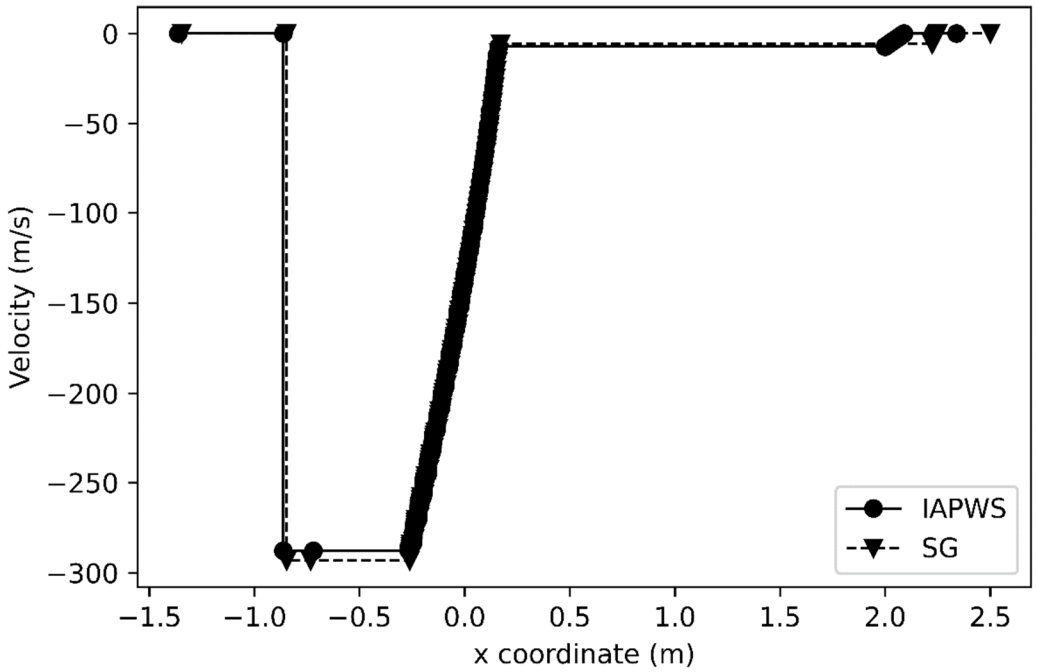

Fig 18 Solution to the Riemann Problem at *t=2.5* ms. Velocity in m/s wrt *x* (m).

Other Cases

We give first an example on Fig 19 where we select $\{\tau_L = 234.54\ \text{L/kg}, p_L = 0.555\ \text{MPa}\}$ and $\{\tau_R = 1.216\ \text{L/kg}, p_R = 17.75\ \text{MPa}\}$

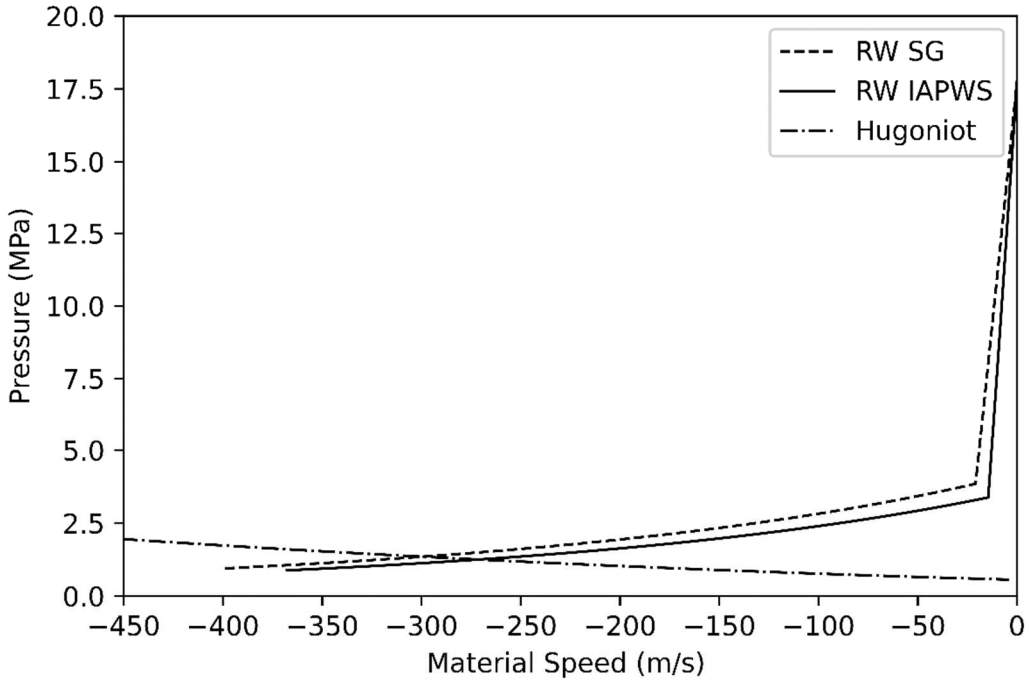

Fig 19 RP with $\{\tau_L = 234\ \text{L/kg}, p_L = 0.555\ \text{MPa}\}\{\tau_R = 1.216\ \text{L/kg}, p_R = 17.75\ \text{MPa}\}$

We compare the IAPWS solution with the SG solution ($\gamma = 2.79$, $p_\infty = 186$): the discrepancy is noticeable. The reason is that with such a low value of τ_R the sound speed is high (~ 1200 m/s) and the parameters of our SG EOS would be more convenient for 850 m/s.

Finally, we show on Fig 20 a case where the initial velocity is $u_R = -300$ m/s . This is still a Riemann Problem but no more a shock tube problem. The Hugoniot curve is made of a blue part in the diphasic domain and a yellow one in the liquid domain. This Hugoniot curve is duplicated from the one plotted in Fig 14. We note that the Hugoniot curve and the rarefaction curve cross each other in the liquid domain for the Hugoniot curve, so that this is a case where the shock makes the fluid to jump directly from a diphasic to a liquid state.

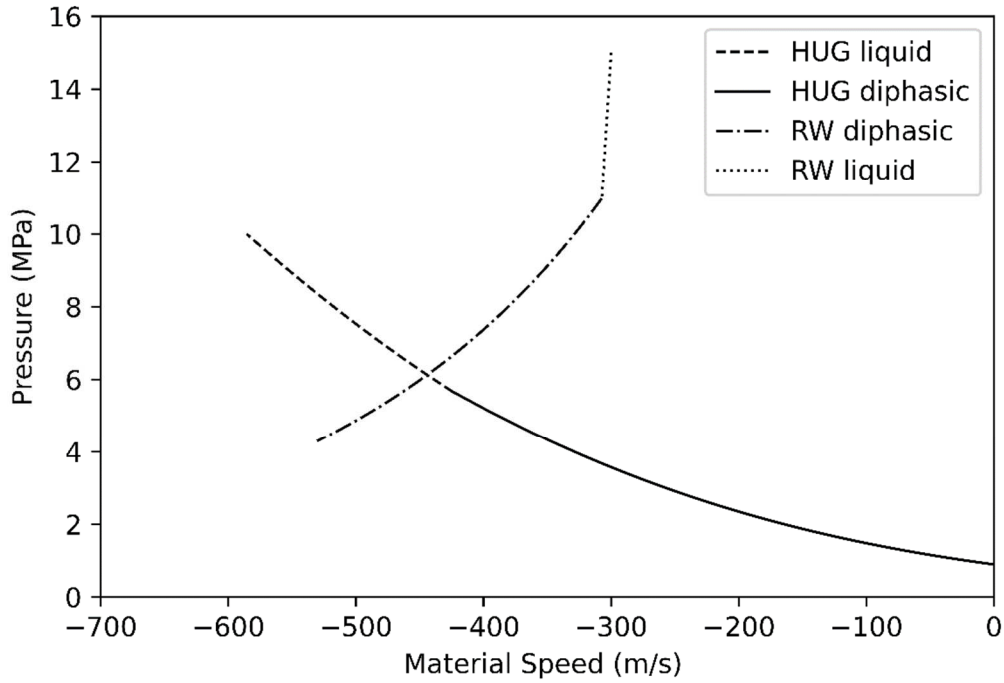

Fig 20 Case $\{\tau_L = 39\,\mathrm{L/kg}, p_L = 0.894\ \mathrm{MPa}, u_L = 0\}$
$\{\tau_R = 1.475\ \mathrm{L/kg}, p_R = 15\ \mathrm{MPa}, u_R = -300\ \mathrm{m/s}\}$

6. Conclusion:

IAPWS97 is a reference equation of state for water. To save computing time in finite difference or finite volume computations, it is possible, at least for temperatures not larger than 623 K, to use computationally more efficient equations of state without losing accuracy.

In the present paper, we have selected a stiffened gas EOS in the liquid domain (IAPWS region 1), a tabulated EOS in the diphasic domain and a perfect gas EOS in the steam domain (IAPWS region 2). However, for the sake of accuracy, it is recommended to carefully select the parameters γ and p_∞.

Acknowledgement: The author is grateful to Alain Forestier for many fruitful exchanges.

Data availability : Data will be made available on reasonable request.
Competing Interests : None
Funding : No funding has been received for this study which I made by myself.

References

[1] T. BARBERON, Ph. HELLUY, Finite volume simulation of cavitating flows, Computers & Fluids 34 (2005) 832–858 ; https://hal.archives-ouvertes.fr/hal-00139597

[2] COROT T. Numerical simulation of shock waves in a bi-fluid flow: application to steam explosion. PhD thesis, Conservatoire national des arts et métiers - CNAM, 2017.

[3] COROT T., MERCIER B., A new nodal solver for the two-dimensional Lagrangian hydrodynamics, J. Computational Physics 353 (2018)1-25. https://dl.acm.org/doi/abs/10.1016/j.jcp.2017.09.053

[4] DESPRÉS B. Numerical Methods for Eulerian and Lagrangian Conservation Laws Springer International Publishing, 2017 https://link.springer.com/book/10.1007/978-3-319-50355-4

[5] G. FACCANONI. Étude d'un modèle fin de changement de phase liquide-vapeur. PhD thesis, École Polytechnique, 2009

[6] Gloria Faccanoni, Samuel Kokh, Grégoire Allaire. "Numerical Simulation with Finite Volume of Dynamic Liquid-Vapor Phase Transition."
FVCA5, Jun 2008, Aussois, France. pp.391-398. HAL-00976927

[7] P. HELLUY. "Simulation numérique des écoulements multiphasiques : de la théorie aux applications". Habilitation à diriger des recherches. Université du Sud
Toulon Var, 2005. URL: https://tel.archives-ouvertes.fr/tel-00657839.

[8] MENIKOFF R., PLOHR B., Riemann Problem for fluid flow of real materials, Rev. Mod. Phys. 61 (1989) 75-130. https://doi.org/10.1103/RevModPhys.61.75

[9] MENIKOFF R., Applications of non-reactive compressible fluids (2001) LANL technical report.

[10] B. Mercier, D. Yang, Z. Zhuang, J. Liang, A simplified analysis of the Chernobyl accident, EPJ Nuclear Sci. Technol. 7, 1 (2021) https://hal.archives-ouvertes.fr/hal-03117177/document

[11] MULLER, S., & VOSS, A. (2006). The Riemann Problem for the Euler Equations with Nonconvex and Non smooth Equation of State: Construction of Wave Curves. SIAM Journal on Scientific Computing, 28(2), 651. https://doi.org/10.1137/040619909

[12] L. Quibel, Simulation of water-vapor two-phase flows with non-condensable gas., PhD thesis, 2020, https://tel.archives-ouvertes.fr/tel-02941486v3

[13] Saurel, R., Cocchi, J. P. & Butler, P. B. A numerical study of cavitation in the wake of a hypervelocity underwater projectile. J. Propulsion Power 15, (1999) 513–522. DOI:10.2514/2.5473 Corpus ID: 120958195

[14] W. WAGNER and H.-J. KRETZSCHMAR. International Steam Tables: Properties of Water and Steam Based on the Industrial Formulation IAPWS-IF97. Springer-Verlag Berlin Heidelberg, 2008. ISBN: 9783540742340. DOI : http://dx.doi.org/10. 1007/978-3-540-74234-0.